

MIT Open Access Articles

*Pyruvate kinase M2-specific siRNA
induces apoptosis and tumor regression*

The MIT Faculty has made this article openly available. **Please share** how this access benefits you. Your story matters.

Citation: Goldberg, M. S., and P. A. Sharp. "Pyruvate Kinase M2-specific siRNA Induces Apoptosis and Tumor Regression." *Journal of Experimental Medicine* 209.2 (2012): 217–224. Web. 3 May 2012.

As Published: <http://dx.doi.org/10.1084/jem.20111487>

Publisher: Rockefeller University Press, The

Persistent URL: <http://hdl.handle.net/1721.1/70493>

Version: Final published version: final published article, as it appeared in a journal, conference proceedings, or other formally published context

Terms of use: Creative Commons Attribution-Noncommercial-Share Alike 3.0 Unported



Pyruvate kinase M2-specific siRNA induces apoptosis and tumor regression

Michael S. Goldberg¹ and Phillip A. Sharp^{1,2}

¹Koch Institute for Integrative Cancer Research, ²Department of Biology, Massachusetts Institute of Technology, Cambridge, MA 02139

The development of cancer-specific therapeutics has been limited because most healthy cells and cancer cells depend on common pathways. Pyruvate kinase (PK) exists in M1 (PKM1) and M2 (PKM2) isoforms. PKM2, whose expression in cancer cells results in aerobic glycolysis and is suggested to bestow a selective growth advantage, is a promising target. Because many oncogenes impart a common alteration in cell metabolism, inhibition of the M2 isoform might be of broad applicability. We show that several small interfering (si) RNAs designed to target mismatches between the M2 and M1 isoforms confer specific knockdown of the former, resulting in decreased viability and increased apoptosis in multiple cancer cell lines but less so in normal fibroblasts or endothelial cells. In vivo delivery of siPKM2 additionally causes substantial tumor regression of established xenografts. Our results suggest that the inherent nucleotide-level specificity of siRNA can be harnessed to develop therapeutics that target isoform-specific exons in genes exhibiting differential splicing patterns in various cell types.

Although much effort in the field of oncology has focused on canonical oncogenes and tumor suppressor genes, the importance of cancer cell metabolism is growing in appreciation (DeBerardinis et al., 2008; Vander Heiden et al., 2009). Known as the Warburg effect (Warburg 1956), this reprogramming of gene expression that alters glucose metabolism enables cells to suppress apoptotic signaling, to grow in hypoxic environments, and to use more glucose for anabolic processes rather than oxidative phosphorylation, even when oxygen is not limiting (Ferguson and Rathmell, 2008).

Pyruvate kinase (PK) catalyzes the conversion of phosphoenolpyruvate (PEP) and ADP to pyruvate and ATP and regulates glucose carbon flux in the cell. In addition to the liver (L) and red blood cell (R) isoforms, two isoforms of pyruvate kinase are found in mammals: M1, which is expressed in most adult tissues, and M2, which is expressed predominantly in embryonic tissue and tumors (Jurica et al., 1998). PKM1 and PKM2 differ by only 23 amino acids within a 56-residue alternatively spliced exon (9 or 10, respectively; Noguchi et al., 1986). These amino acids in the M2 isoform constitute an allosteric pocket unique to PKM2 that allows it to bind its activator, fructose 1,6-bisphosphate (FBP), and be regulated by phosphotyrosine-based growth signals (Dombrackas et al., 2005; Christofk et al., 2008b).

Pyruvate kinase activity can be modulated not only by alternative splicing (Clower et al., 2010; David et al., 2010) but also by allostery (Boxer et al., 2010; Vander Heiden et al., 2010a). PKM2 exists as either an active tetramer or a relatively inactive dimer or monomer. The latter form is commonly expressed at high levels in tumor cells (Ugurel et al., 2005), and this conformation is favored by binding of phosphotyrosinated proteins, which displace FBP, the glycolytic metabolite that induces formation of the tetrameric form (Ashizawa et al., 1991). The low activity of the monomer and dimer forms causes an accumulation of PEP and other glycolytic intermediates, resulting in the redirection of glucose to serve as a carbon source for macromolecule biosynthesis, which is important for cell division (Christofk et al., 2008a).

Recently, it was shown that cancer cells use an alternative glycolytic pathway (Vander Heiden et al., 2010b). Specifically, the decreased pyruvate kinase activity associated with PKM2 expression allows PEP-dependent histidine phosphorylation of the upstream glycolytic enzyme phosphoglycerate mutase, decoupling generation of ATP

CORRESPONDENCE

Phillip A. Sharp:
sharp@mit.edu

Abbreviations used: FBP, fructose 1,6-bisphosphate; PEP, phosphoenolpyruvate; PK, pyruvate kinase.

© 2012 Goldberg and Sharp. This article is distributed under the terms of an Attribution-Noncommercial-Share Alike-No Mirror Sites license for the first six months after the publication date (see <http://www.rupress.org/terms>). After six months it is available under a Creative Commons License (Attribution-Noncommercial-Share Alike 3.0 Unported license, as described at <http://creativecommons.org/licenses/by-nc-sa/3.0/>).

from PEP-mediated phosphotransfer. The level of PKM2 expression might be important in balancing the two glycolytic pathways. We find that targeting with a PKM2-specific small interfering (si) RNA inhibits the growth of many cancer cell lines.

The knockdown of pyruvate kinase by shRNA targeting sequences common to both the M1 and M2 isoforms resulted in decreased rates of glucose metabolism and reduced cell proliferation (Christofk et al., 2008a). Although rescue of PKM2 enhances tumor growth, the effect of knocking down PKM2 specifically has yet to be investigated. To this end, we designed siRNAs that are specific to PKM2 and examined their ability to confer specific knockdown, to decrease cell proliferation, to induce apoptosis, and to inhibit tumor xenograft growth.

RESULTS AND DISCUSSION

Identification of M2-specific siPKs

Sequences that would target the M2 isoform of pyruvate kinase specifically were identified (Fig. 1 A). A custom library of siRNAs that tiled exon 10, which is included exclusively in the M2 isoform, was screened (Table S1). The ability of each siRNA to decrease cell viability in the human colon cancer cell line HCT116 was assessed (Fig. 1 B). Notably, very few siRNAs (<7%) actually generated a phenotype, as defined by <20% survival relative to untreated cells. Three sequences from the tiling library—si27, si155, and si156—conferred a particularly potent inhibition of survival or proliferation (<5% survival). The ability to inhibit proliferation was observed to correlate with the extent of target knockdown, supporting an on-target effect.

siControl, a sequence that targets firefly luciferase, was used as a negative control. siPK, a commercially available sequence which targets both PKM1 and PKM2, was used as a positive control. To maximize the specificity of the library, ON-TARGETplus siRNAs were used to reduce off-target effects (Jackson et al., 2006). Specifically, the sense strand is modified to prevent interaction with RISC and favor antisense strand uptake, and the antisense strand seed region is modified to minimize seed-related off targeting.

To demonstrate that the effects imparted by the most efficacious siRNAs were a result of the knockdown of the M2 isoform and not to the knockdown of PKM1, isoform-specific real-time PCR was performed using primers that were designed to amplify either isoform individually or total pyruvate kinase (Fig. 2 A). The knockdown of PKM2 was both specific and robust for si27, si155, and si156. As expected, siPK resulted in potent knockdown of both PKM1 and PKM2. The pronounced changes at the mRNA level indicate that there is efficient uptake of siRNA.

siPKM2 induces apoptosis specifically in cancer cell lines

Next, the effect of the three most active siRNAs on viability and apoptosis was examined in HCT116, HepG2, and SKOV3 cells (Fig. 2, B and C). HepG2, a hepatocellular carcinoma cell line, and SKOV3, an ovarian carcinoma cell line, were selected to complement HCT116, in which the original screen had been performed, because the current most advanced siRNA delivery systems successfully deliver RNAi therapeutics to the

liver (Akinc et al., 2008; Love et al., 2010) and ovaries (Huang et al., 2009; Goldberg et al., 2011) in vivo.

The primary screen used a luminescent assay in which the signal was proportional to the amount of ATP present, a surrogate for viability. To measure the number of intact viable cells directly, a fluorogenic, cell-permeant peptide substrate was used as a complementary assay. Viability and Caspase3/7-mediated apoptosis were measured in all three cell lines. Although their relative efficacy varies slightly between cell lines, si27, si155, and si156 consistently reduce cell viability and increase apoptosis in each cancer line examined, whereas the negative control does not. That three independent sequences targeting the M2 isoform confer the same phenotype supports the specificity of the effect, as each was confirmed to impart robust silencing of the target gene. Importantly, these data indicated that the decreased relative viability is mostly attributable to programmed cell death rather than simply to inhibition of proliferation. Progressing toward in vivo studies, we elected to focus on si156, because it was among the most active in all cell lines tested.

Real-time PCR was used to confirm that the knockdown was robust and specific and was correlated to phenotype. A direct proportionality between knockdown and efficacy was observed. The minimum knockdown required for efficacy was shown to be rather high. An ~90% mRNA silencing (2.5 nM) was required to observe a 50% decrease in cell viability. A >95% mRNA silencing (5 nM) conferred a >95% decrease in HCT116 cell viability (Fig. 2 D). That strong silencing is required to impart a phenotype is supported by previous efforts to inhibit PKM2 activity specifically with small molecules, which proved difficult (Vander Heiden et al., 2010a). With no effect on PKM1 levels, si156 conferred as much as a 97% knockdown of PKM2 mRNA at a dose of 5 nM. It was additionally confirmed that this knockdown at the mRNA level translated to knockdown at the protein level (Fig. 2 E). Although the levels of PKM1 could not be measured directly, as an antibody against this protein was not commercially available, total PK was reduced in HCT116, HepG2, and SKOV3 cells treated with si156, and PKM2 was specifically knocked down in all of these cell lines. Moreover, the knockdown resulted in a twofold decrease in lactate production, providing functional biochemical support for an on-target effect (Fig. 2 F). The residual lactate production is probably attributable to the presence of either the M1 isoform or residual PKM2 protein.

The NCI-60 is a panel of human tumor cell lines that are well characterized and broadly used in drug screening. The constituent lines represent multiple types of cancer, including brain, breast, colon, lung, ovarian, renal, and skin cancers, and sundry underlying genetic insults, including K-ras, B-Raf, and PIK3CA activation as well as p53, p16, and PTEN inactivation. Microarray data show that the cell lines used have a wide range of PKM2 expression levels, from relatively low (HCT-15, T47D) to relatively high (IGROV-1, U251) (<http://dtp.cancer.gov/mtweb>).

To confirm that the effects of si156 on cell viability are not highly dependent on the type of causal mutations, 10 cell lines from the NCI-60 were treated with siControl or si156, and the effects of the siRNAs on viability and Caspase3/7-mediated

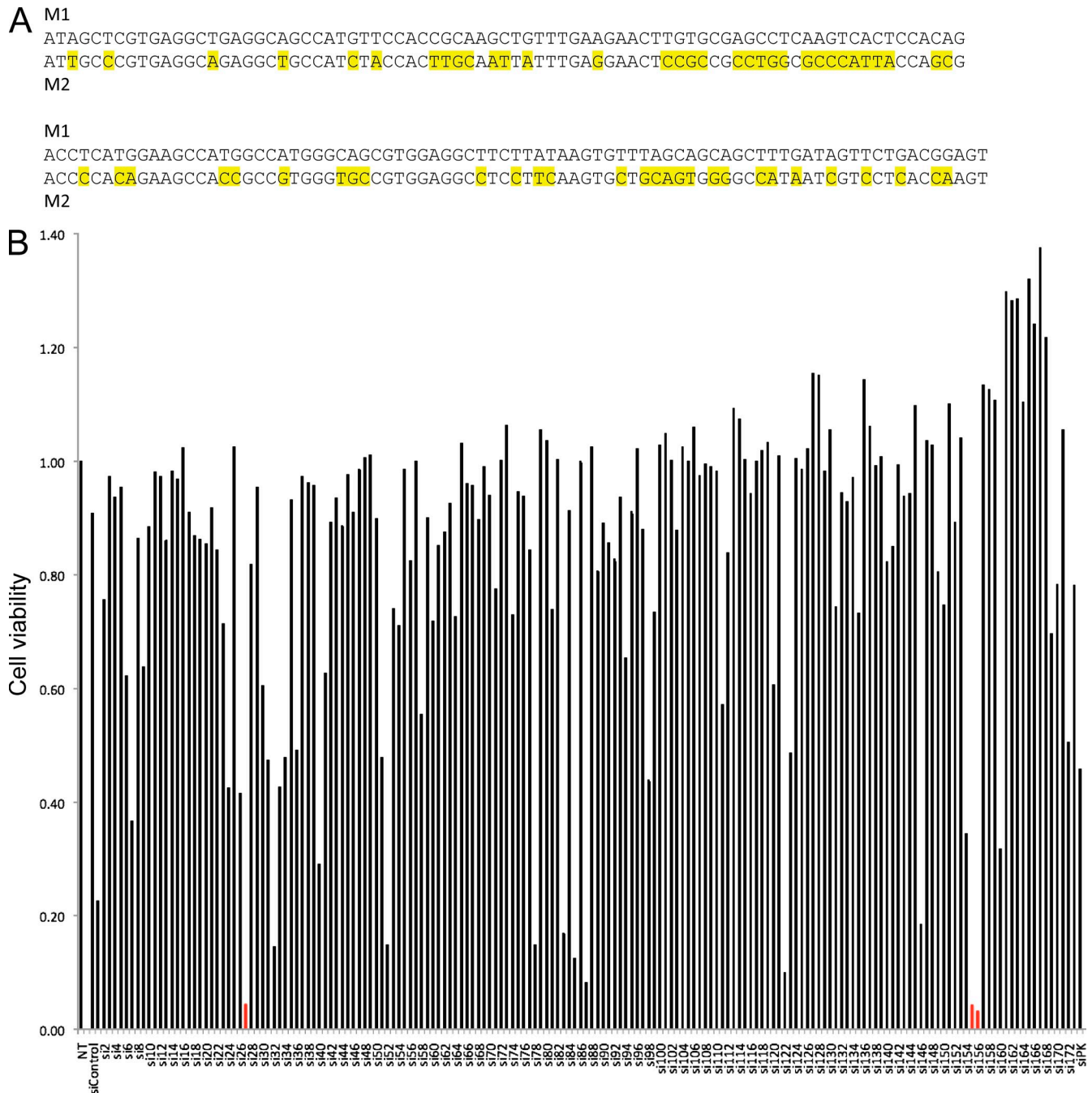


Figure 1. The screening of a tiling siRNA library reveals sequences that can discriminate between the M1 and M2 isoforms of pyruvate kinase.

(A) The sequences of the M1 and M2 isoforms of pyruvate kinase are shown. Mismatches are highlighted in yellow. (B) The viability of HCT116 cells for each member of the siPKM2 library is shown relative to the no treatment control. Cells were transfected with 5 nM siRNA at 0, 48, and 96 h and were assayed after 6 d. Transfections were performed in technical quadruplicate on two independent occasions. The three most active siRNA sequences are highlighted in red. NT, no treatment.

apoptosis were determined (Fig. 3, A and B). In all 10 cell lines, viability is drastically reduced among the cells treated with si156 relative to those treated with siControl, and it is confirmed that the decreased viability is mostly attributable to the induction of apoptosis, regardless of the cells' growth rates. The extent of apoptotic induction varies between the cell lines, but up-regulation of apoptosis was observed in all cases.

Importantly, we tested whether the effect of si156 on viability is specific to cancer cell lines. Adult skin fibroblasts and human umbilical vein endothelial cells were grown in vitro at low passage number and transfected with siControl or si156. Unlike most differentiated cells, these primary cells actively proliferate in vitro and express PKM2. We sought to verify that the M2 isoform was being specifically knocked down at

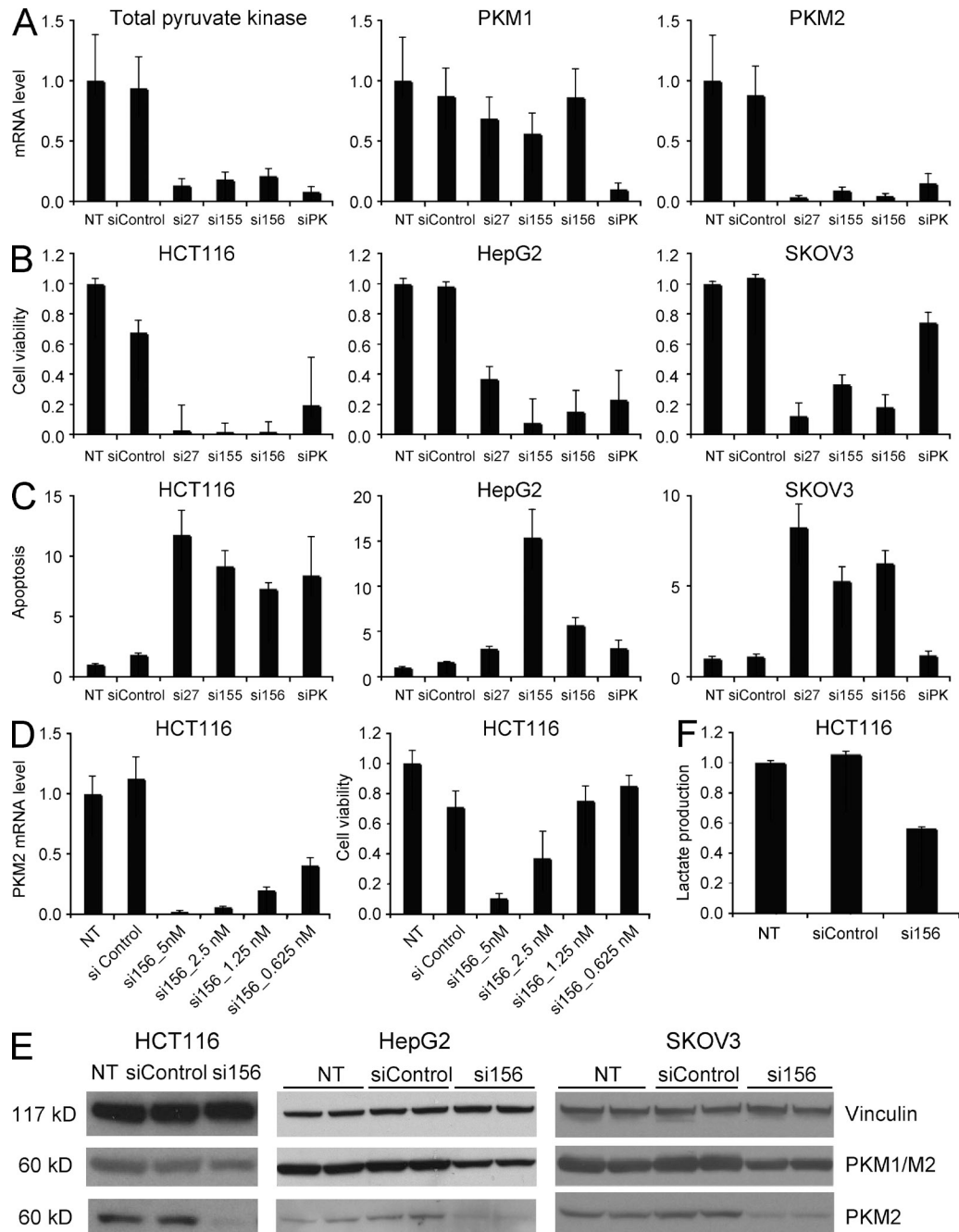


Figure 2. The knockdown of the M2 isoform of pyruvate kinase mRNA by si27, si155, and si156 is potent and specific. (A) HCT116 cells were transfected with 5 nM siRNA. Duplicate biological samples were collected 48 h after transfection. Quantitative real-time PCR primers were designed to amplify total PKM, PKM1 only, or PKM2 only from HCT116 total RNA. HCT116, HepG2, and SKOV3 cells were transfected with 5 nM siRNA at 0, 48, and 96 h. (B and C) Cells were assayed for cell viability (B) and apoptosis (C) after 6 d. Results are normalized relative to the no treatment control. Transfections were performed in technical triplicate on two independent occasions. NT, no treatment; siPK, siRNA targeting both M1 and M2 isoforms; siControl, siRNA targeting firefly luciferase. Error bars denote standard deviation. (D) HCT116 cells were transfected with serial dilutions of si156 at 0, 48, and 96 h. Cells were assayed for cell viability after 6 d. Results are normalized relative to the no treatment control. Transfections were performed in technical quadruplicate on two independent occasions. Error bars denote standard deviation. (E) Lysates were collected from HCT116, HepG2, and SKOV3 cells 48 h after transfection with 5 nM siRNA. Blots were probed with antibodies targeting either total PKM or PKM2. Duplicate biological samples were collected for HepG2 and SKOV3, the cell lines used in the xenograft experiment. NT, no treatment. Vinculin was used as a loading control. (F) Effect of si156 on lactate production in HCT116 cells. The assay was performed 48 h after cells were transfected with 5 nM siRNA. Results are normalized to the no treatment control, and lactate production is further normalized to cell number. The experiment was performed in biological and technical duplicate on two independent occasions. Error bars denote standard deviation.

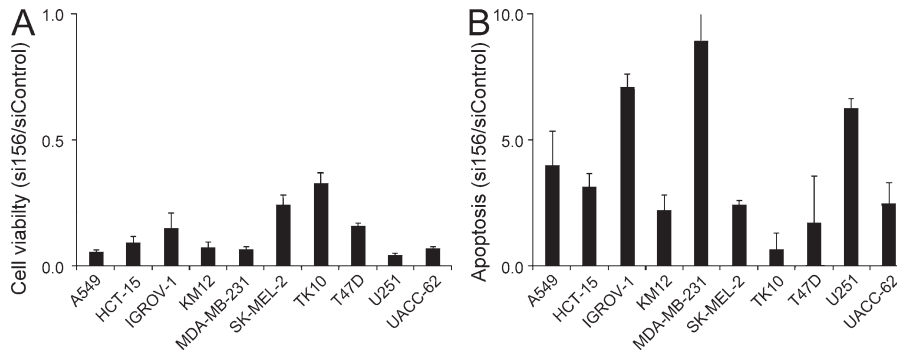


Figure 3. Cancer cells are addicted to metabolic reprogramming by PKM2. 10 members of the NCI-60, representing multiple types of cancer and numerous underlying genetic insults, were transfected with 5 nM siControl or si156 at 0, 48, and 96 h. Cell viability (A) and apoptosis (B) were determined after 6 d. Results are normalized to the no treatment control, and apoptosis is further normalized to cell number. Transfections were performed in technical quadruplicate on two independent occasions. NT, no treatment. Error bars denote standard deviation.

the mRNA level (Fig. 4 A). Notably, despite the presence of PKM2 knockdown, which was also confirmed at the protein level (Fig. 4 B), an examination of cell viability revealed that treatment with si156 did not have a detrimental effect on survival for these noncancerous cells (Fig. 4 C). It is possible that after silencing of PKM2, the level of expression of PKM1 in normal cells is adequate for viability, whereas this is not the case for transformed cells. Alternatively, evidence is emerging that there are noncatalytic roles for PKM2 in the cell, including activation of VEGF (Semenza, 2011). Cancer cells may be more sensitive to these perturbations than normal cells. The extent of silencing at the mRNA level is comparable between HCT116 cancer cells and SF372 adult fibroblasts, yet

the phenotype of decreased cell growth is observed only in the former. Thus, the difference in phenotype is owing to the inherent biology of the cell types rather than the inability of the siRNA to impart posttranscriptional gene silencing.

siPKM2 leads to regression of tumor volume

A member of the lipid-like class of materials dubbed lipiods (Akinc et al., 2008) was used to encapsulate and deliver siRNA as nanoparticles to the xenograft tumors. The selected lipiod, 98N₁₂-5(1), has previously been shown to knock down multiple hepatic genes (Akinc et al., 2008) as well as a putative oncogene *in vivo*, resulting in reduction of tumor volume and extension of survival in three mouse models of ovarian cancer (Huang et al., 2009; Goldberg et al., 2011).

We evaluated the efficacy of the siRNA treatments *in vivo* using xenograft models of liver (HepG2) and ovarian (SKOV3) carcinomas that were injected subcutaneously in SCID mice. When the induced tumors were ~200 mm³ in volume, the mice were randomly divided

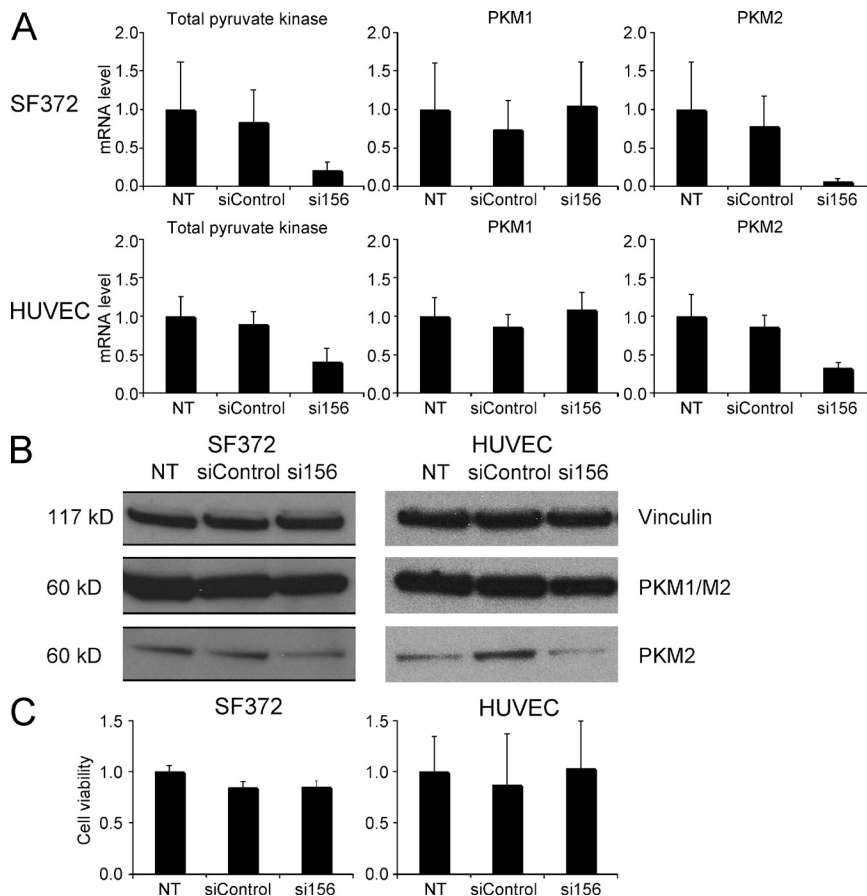


Figure 4. si156 does not reduce the viability of normal human primary cells. (A) The knockdown of the M2 isoform of pyruvate kinase mRNA by si156 is confirmed in SF372 human adult skin fibroblasts and human umbilical vein endothelial cells (HUVECs). Primers were designed to amplify total PKM, PKM1 only, or PKM2 only. Duplicate biological samples were collected 48 h after transfection with 5 nM siRNA, and each sample was assayed in technical triplicate. (B) Lysates were collected from SF372 and HUVEC cells 48 h after transfection with 5 nM siRNA. Blots were probed with antibodies targeting either total PKM or PKM2. NT, no treatment. Vinculin was used as a loading control. (C) Relative cell viability was determined after six days. SF372 and HUVEC cells were transfected with 5 nM siRNA at 0, 48, and 96 h. Transfections were performed in technical quadruplicate on two independent occasions. NT, no treatment. Error bars denote standard deviation.

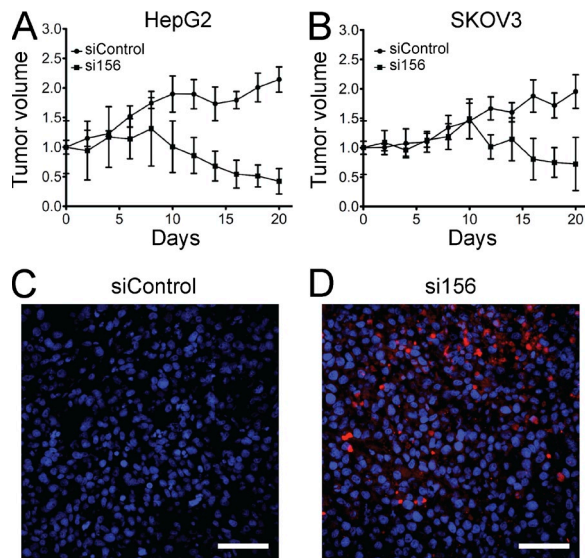


Figure 5. Administration of lipidoid-formulated si156 results in a reduction in volume of established tumors. (A) HepG2. (B) SKOV3. Error bars denote SEM ($n = 4$). The size difference between the treatment and control groups is significant by two-tailed Student's t test at day 20. $P = 0.0005$ and $P = 0.0133$, respectively. (C and D) TUNEL staining confirms induction of apoptosis *in vivo*. Sections of SKOV3 tumors from mice treated with lipidoid-formulated siControl (C) or si156 (D) are shown. Blue, DAPI; red, TUNEL. Bars, 250 μm .

into separate groups and treated intratumorally twice per week for a period of 3 wk with either siControl or si156. Local administration was used to ensure effective delivery.

Compared with the control treatment, si156 showed activity against established xenograft tumors. Tumor regression was observed after two to three doses (~ 10 d) for tumors receiving the siPKM2 treatment. The trial was halted when the control group had to be euthanized. At the end of the trial (day 20, six treatments), the mean \pm SD ($n = 4$) tumor volumes were 541 ± 107 and 83 ± 84 mm³ for HepG2 tumors and 348 ± 102 and 88 ± 110 mm³ for SKOV3 tumors for siControl and si156, respectively (Fig. 5, A and B).

Treatment with si156 prevented tumor expansion and even resulted in a volume reduction. Indeed, nearly all of the measured volume in the siPKM2-treated mice could be attributed to scar tissue caused by the intratumoral injections, as determined by attempted tumor recovery after the animals were sacrificed. There was no remnant of HepG2 tumor in half of the si156-treated animals, and there was no remnant of SKOV3 tumor in three quarters of the si156-treated animals. In the latter case, recovered tumor tissue was sectioned and visualized by TUNEL staining (Fig. 5 C). si156-treated tumors displayed significantly higher levels of apoptosis.

Finally, to confirm that the effect was mediated specifically by the RNAi pathway and not by an innate immune response (Kleinman et al., 2008), which can be sequence specific (Hornung et al., 2005), serum was collected from SCID mice treated with PBS, formulated siControl, or formulated si156, and interferon- α levels were examined by ELISA. All samples

fell below the standard curve and matched baseline levels, indicating that the observed effect was not conferred by an interferon-induced stimulation of an immune response.

siPKM2 is an example of isoform-specific RNAi

Although multiple available siRNA design algorithms did not predict any sequences within alternative exon 10 that would mediate robust silencing, we have identified multiple siRNAs that afford potent and specific silencing of the M2 isoform of pyruvate kinase. An inspection of the 10 top performing sequences reveals that the number of mismatches between the M1 and M2 isoforms ranges from 4 to 13. 5 of these 10 sequences contain mismatches at one of the critical central positions 10 or 11, which have been shown to be important in conferring specificity (Wang et al., 2008b). We observed one "hot spot": two of the top three siRNAs target consecutive 19-mers (si155 and si156). We also observed one "warm spot": three siRNAs work moderately well over a sequence that spans 23 nucleotides (si83, si85, and si87).

Recent analysis of transcriptomes indicates that $>90\%$ of all human genes are expressed as alternatively spliced isoforms (Wang et al., 2008a). The ability to target one isoform of a gene effectively is inherent of siRNA technology. This work represents the first specific siRNA targeting of the M2 isoform of pyruvate kinase at the mRNA level and demonstrates that this knockdown can induce caspase-mediated apoptosis. The combination of shPK and chemotherapy has been reported to increase the efficacy of the latter (Shi et al., 2010; Guo et al., 2011). These studies, however, used a sequence that targets both the M1 and M2 isoforms. As a consequence, the results of these studies cannot be attributed specifically to M2 knockdown.

A small molecule drug that targets pyruvate dehydrogenase kinase was reported to affect cancer cell metabolism (Bonnet et al., 2007), confirming that metabolic modulation may be a viable therapeutic approach in the treatment of glioblastoma (Michelakis et al., 2010). Notably, small molecule antagonists of FBP binding by PKM2 may be insufficient to provide a complete abrogation of the role of PKM2 in cancer, as PKM2 has been demonstrated to interact and cooperate with Oct-4 to regulate transcription in a manner that is seemingly unrelated to metabolism (Lee, et al., 2008). Indeed, PKM2 appears to have noncatalytic roles in the cell (Mazurek, 2011), so silencing PKM2 with siRNA may have therapeutic effects beyond that possible with a small molecule.

Off-target effects as a result of miRNA-type targeting are not likely to be responsible for the observed effects. Multiple sequences—containing different seed regions—addressing the same target were shown to confer the same phenotype in cancer cell lines. Furthermore, the extent of induction of apoptosis roughly correlated with the degree of knockdown. The knockdown was shown to repress lactate production, confirming that the siRNA modulated metabolism. The siRNAs included chemical modifications that have been shown to minimize off-target effects. Immunostimulation was not implicated in the observed tumor regression and certainly could not account for the specific inhibition in cell culture.

Previous work demonstrated that the M2 isoform of pyruvate kinase is important for cancer metabolism and tumor growth (Christofk et al., 2008a), suggesting that it might be a good drug target. We have illustrated that it can be effectively targeted in a specific manner by siRNA and that this targeting induces apoptosis in cancer cell lines. It is noteworthy that glioblastoma cells (U251), which are known to retain high expression of the more efficient M1 isoform (Clower et al., 2010; David et al., 2010), also undergo apoptosis when the M2 isoform is knocked down despite the fact that they should still have efficient glycolytic flux through the action of the M1 isoform. This contrasts with the study reporting that expression of the M1 isoform is sufficient to rescue tumor formation, wherein tumor growth simply occurred at a slower rate than when the M2 isoform was expressed (Christofk et al., 2008a).

This work illustrates an example of the utility of RNAi in discriminating between closely related enzyme isoforms at the nucleotide level that may be difficult to achieve by traditional approaches. Several findings are worthy of emphasis. It is surprising that inhibiting the production of an enzyme that contributes to a pro-proliferative phenotype owing to its decreased activity should result in apoptosis. Finally, the findings are generalizable across divergent tumor types and etiologies. The results suggest that most tumor cells have pathways that converge on this node.

MATERIALS AND METHODS

Cell culture. Cells were maintained at 37°C and 5% CO₂ in Dulbecco's modified Eagle medium or RPMI-1640 supplemented with L-glutamine, penicillin/streptomycin, and 10% fetal bovine serum (Hyclone).

siRNA. The custom library was synthesized by Thermo Fisher Scientific as ON-TARGET^{plus} siRNA. The *in vivo* experiments were conducted using standard siRNA.

mRNA quantitation. 15,000 cells per well were seeded in 96-well plates (Falcon) and transfected with 5 nM siRNA using HiPerFect Transfection Reagent (QIAGEN). After 48 h, RNA was collected and reverse transcribed using the Power SYBR Green Cells-to-CT kit (Invitrogen). Real-time PCR was performed on an Applied Biosystems 7500 using the following primer pairs (mismatches between M1 and M2 isoforms are underlined, and Tata binding protein [TBP] was used for normalization): PKM1/M2 forward: 5'-CATTGATTCACCACCCATCA-3'; PKM1/M2 reverse: 5'-AGACGAGCCACATTCATTCC-3'; PKM1 forward: 5'-CGAGCCTCAAGTCACTCCAC-3'; PKM1 reverse: 5'-GTGAGCAGACCTGCCAGACT-3'; PKM2 forward: 5'-ATTATTTGAGGAAGTCCGCCGCT-3'; PKM2 reverse: 5'-ATTCCGGGTCACAGCAATGATGG-3'; TBP forward: 5'-GGA-GAGTTCTGGGATTGTAC-3'; and TBP reverse: 5'-CTTATCCTCATGATTACCGCAG-3'.

Western blot analysis. 250,000 cells per well were seeded in 6-well plates (Falcon) and transfected with 5 nM siRNA using HiPerFect Transfection Reagent (QIAGEN). After 48 h, the cells were lysed, the supernatant was quantitated, and the protein was boiled in 4× SDS sample buffer and run on 4–12% gradient Bis-Tris gels (Invitrogen). Proteins were transferred to nitrocellulose, and Western blots were performed using rabbit monoclonal anti-PKM1/M2 (Cell Signaling Technology), rabbit polyclonal anti-PKM2 (Cell Signaling Technology), and mouse monoclonal anti-Vinculin (Sigma-Aldrich).

Cell viability analysis. 5,000 cells per well were seeded in 96-well plates (Falcon) and transfected with 5 nM siRNA using HiPerFect Transfection Reagent (QIAGEN). Cell viability was determined at 144 h by CellTiter-Glo or GF-AFC (Promega). To retain knockdown of PKM2, siRNA transfection

was repeated at 48 and 96 h. For the NCI-60 cell lines, 2,000 cells were seeded per well.

Assessment of apoptosis. 5,000 cells per well were seeded in 96-well plates (Falcon) and transfected with 5 nM siRNA using HiPerFect Transfection Reagent (QIAGEN). Relative apoptosis was determined at 144 h by Caspase-Glo 3/7 using the Apotax-Glo Assay (Promega). To retain knockdown of PKM2, siRNA transfection was repeated at 48 and 96 h. For the NCI-60 cell lines, 2,000 cells were seeded per well.

Lactate assay. Lactate production was measured using a colorimetric assay kit (BioVision). 150,000 HCE116 cells were seeded in 12-well plates (Corning) and transfected with 5 nM siRNA using HiPerFect Transfection Reagent (QIAGEN). After 48 h, the subconfluent cells were washed three times with PBS. Krebs-Ringer-Hepes buffer supplemented with 10 mM glucose was added, and aliquots of media from each well were assessed 30 min later for the amount of lactate present. The cells were counted with a hemocytometer and by CellTiterGlo to normalize.

In vivo siPKM2 efficacy study. SCID mice (4 wk old) were purchased from Taconic. All *in vivo* experimentation was performed under the supervision of the Division of Comparative Medicine (DCM), Massachusetts Institute of Technology, and in compliance with the Principles of Laboratory Animal Care of the National Institutes of Health. HepG2 and SKOV3 were obtained from American Type Culture Collection.

Anti-tumor efficacy was evaluated in SCID mice induced with HepG2 and SKOV3 tumors on the left and right hind flanks, respectively, with a single s.c. injection of 2.5×10^6 cells. Mice were randomized when the tumors were approximately ~ 200 mm³ in volume and were subjected to treatment with either siControl or si156, formulated with 98N₁₂-5(1) as previously described (Akinc et al., 2008; *n* = 4 per group). The therapy was given in the form of an intratumoral injection twice a week at a dosage of 100 μg (~ 1 mg/kg/100 mm³ tumor volume). Day 0 indicates that start of treatment. Measurements of tumor volume were made every 2 d using the equation: tumor volume = (width² × length)/2. The mice were monitored for up to 22 d and were euthanized when the tumor burden was deemed to be excessive by the DCM. A two-tailed Student's *t* test was used for comparison of tumor sizes.

For histology, tumors were harvested from mice at the end of the trial (day 22), frozen in OCT (−80°C), and cut into 5-μm sections for analysis. Sections were fixed (5% formaldehyde) and permeabilized with cold ethanol (70% volume). TUNEL assay was performed according to the manufacturer's instructions (Invitrogen), and the nuclei were stained with Hoechst. Sections were examined with a DeltaVision confocal (Applied Precision) at 20×.

Immunostimulation study. SCID mice (Taconic) were administered PBS, 98N₁₂-5(1)-formulated siControl, or 98N₁₂-5(1)-formulated si156 at a dosage of 100 μg via subcutaneous injection (*n* = 3 per group). To measure serum interferon-α levels, blood was collected from mice 6 h after injection by cardiac puncture. The level of interferon-α was measured by ELISA according to the manufacturer's protocol (PBL). The assay was performed in biological and technical triplicate.

Online supplemental material. Table S1 lists the tiling siRNA sequences designed to silence PKM2. Every possible 19-mer siRNA containing at least one mismatch between the M1 (exon 9) and M2 (exon 10) isoforms of human pyruvate kinase is represented. Online supplemental material is available at <http://www.jem.org/cgi/content/full/jem.20111487/DC1>.

We dedicate this work to the memories of Terry Fox and Dave Goldberg.

We thank Z. Poon for his assistance with the animal experiments, D. Xing for his assistance with the immunostimulatory assay, the Weinberg Laboratory for sharing adult skin fibroblast cells, the Langer Laboratory for sharing human umbilical vein endothelial cells, the Bhatia Laboratory for sharing members of the NCI-60 cell line panel, and A. Gurtan, A. Ravi, and M. Vander Heiden for providing helpful comments on the manuscript.

This work was supported by an MIT-Harvard Center for Cancer Nanotechnology Excellence Grant U54 CA151884 from the National Cancer Institute, by the Marie D.

& Pierre Casimir-Lambert Fund, and partially by the Cancer Center Support (core) grant P30-CA14051 from the National Cancer Institute.

Competing financial interests: a provisional patent has been filed in relation to this work. The authors have no other conflicting financial interests.

Author contributions: M.S. Goldberg designed and performed the experiments; M.S. Goldberg and P.A. Sharp wrote the manuscript.

Submitted: 19 July 2011

Accepted: 8 December 2011

REFERENCES

- Akinc, A., A. Zumbuehl, M. Goldberg, E.S. Leshchiner, V. Busini, N. Hossain, S.A. Bacallado, D.N. Nguyen, J. Fuller, R. Alvarez, et al. 2008. A combinatorial library of lipid-like materials for delivery of RNAi therapeutics. *Nat. Biotechnol.* 26:561–569. <http://dx.doi.org/10.1038/nbt1402>
- Ashizawa, K., M.C. Willingham, C.M. Liang, and S.Y. Cheng. 1991. In vivo regulation of monomer-tetramer conversion of pyruvate kinase subtype M2 by glucose is mediated via fructose 1,6-bisphosphate. *J. Biol. Chem.* 266:16842–16846.
- Bonnet, S., S.L. Archer, J. Allalunis-Turner, A. Haromy, C. Beaulieu, R. Thompson, C.T. Lee, G.D. Lopaschuk, L. Puttagunta, S. Bonnet, et al. 2007. A mitochondria-K⁺ channel axis is suppressed in cancer and its normalization promotes apoptosis and inhibits cancer growth. *Cancer Cell.* 11:37–51. <http://dx.doi.org/10.1016/j.ccr.2006.10.020>
- Boxer, M.B., J.K. Jiang, M.G. Vander Heiden, M. Shen, A.P. Skoumbourdis, N. Southall, H. Veith, W. Leister, C.P. Austin, H.W. Park, et al. 2010. Evaluation of substituted N,N'-diarylsulfonamides as activators of the tumor cell specific M2 isoform of pyruvate kinase. *J. Med. Chem.* 53:1048–1055. <http://dx.doi.org/10.1021/jm901577g>
- Christofk, H.R., M.G. Vander Heiden, M.H. Harris, A. Ramanathan, R.E. Gerstzen, R. Wei, M.D. Fleming, S.L. Schreiber, and L.C. Cantley. 2008a. The M2 splice isoform of pyruvate kinase is important for cancer metabolism and tumour growth. *Nature.* 452:230–233. <http://dx.doi.org/10.1038/nature06734>
- Christofk, H.R., M.G. Vander Heiden, N. Wu, J.M. Asara, and L.C. Cantley. 2008b. Pyruvate kinase M2 is a phosphotyrosine-binding protein. *Nature.* 452:181–186. <http://dx.doi.org/10.1038/nature06667>
- Clower, C.V., D. Chatterjee, Z. Wang, L.C. Cantley, M.G. Vander Heiden, and A.R. Krainer. 2010. The alternative splicing repressors hnRNP A1/A2 and PTB influence pyruvate kinase isoform expression and cell metabolism. *Proc. Natl. Acad. Sci. USA.* 107:1894–1899. <http://dx.doi.org/10.1073/pnas.0914845107>
- David, C.J., M. Chen, M. Assanah, P. Canoll, and J.L. Manley. 2010. HnRNP proteins controlled by c-Myc deregulate pyruvate kinase mRNA splicing in cancer. *Nature.* 463:364–368. <http://dx.doi.org/10.1038/nature08697>
- DeBerardinis, R.J., J.J. Lum, G. Hatzivassiliou, and C.B. Thompson. 2008. The biology of cancer: metabolic reprogramming fuels cell growth and proliferation. *Cell Metab.* 7:11–20. <http://dx.doi.org/10.1016/j.cmet.2007.10.002>
- Dombrauckas, J.D., B.D. Santarsiero, and A.D. Mesecar. 2005. Structural basis for tumor pyruvate kinase M2 allosteric regulation and catalysis. *Biochemistry.* 44:9417–9429. <http://dx.doi.org/10.1021/bi0474923>
- Ferguson, E.C., and J.C. Rathmell. 2008. New roles for pyruvate kinase M2: working out the Warburg effect. *Trends Biochem. Sci.* 33:359–362. <http://dx.doi.org/10.1016/j.tibs.2008.05.006>
- Goldberg, M.S., D. Xing, Y. Ren, S. Orsulic, S.N. Bhatia, and P.A. Sharp. 2011. Nanoparticle-mediated delivery of siRNA targeting Parp1 extends survival of mice bearing tumors derived from Brca1-deficient ovarian cancer cells. *Proc. Natl. Acad. Sci. USA.* 108:745–750. <http://dx.doi.org/10.1073/pnas.1016538108>
- Guo, W., Y. Zhang, T. Chen, Y. Wang, J. Xue, Y. Zhang, W. Xiao, X. Mo, and Y. Lu. 2011. Efficacy of RNAi targeting of pyruvate kinase M2 combined with cisplatin in a lung cancer model. *J. Cancer Res. Clin. Oncol.* 137:65–72. <http://dx.doi.org/10.1007/s00432-010-0860-5>
- Homung, V., M. Guenther-Biller, C. Bourquin, A. Ablasser, M. Schlee, S. Uematsu, A. Noronha, M. Manoharan, S. Akira, A. de Fougerolles, et al. 2005. Sequence-specific potent induction of IFN- α by short interfering RNA in plasmacytoid dendritic cells through TLR7. *Nat. Med.* 11:263–270. <http://dx.doi.org/10.1038/nm1191>
- Huang, Y.H., Y. Bao, W. Peng, M. Goldberg, K. Love, D.A. Bumcrot, G. Cole, R. Langer, D.G. Anderson, and J.A. Sawicki. 2009. Claudin-3 gene silencing with siRNA suppresses ovarian tumor growth and metastasis. *Proc. Natl. Acad. Sci. USA.* 106:3426–3430. <http://dx.doi.org/10.1073/pnas.0813348106>
- Jackson, A.L., J. Burchard, D. Leake, A. Reynolds, J. Schelter, J. Guo, J.M. Johnson, L. Lim, J. Karpilow, K. Nichols, et al. 2006. Position-specific chemical modification of siRNAs reduces “off-target” transcript silencing. *RNA.* 12:1197–1205. <http://dx.doi.org/10.1261/rna.30706>
- Jurica, M.S., A. Mesecar, P.J. Heath, W. Shi, T. Nowak, and B.L. Stoddard. 1998. The allosteric regulation of pyruvate kinase by fructose-1,6-bisphosphate. *Structure.* 6:195–210. [http://dx.doi.org/10.1016/S0969-2126\(98\)00021-5](http://dx.doi.org/10.1016/S0969-2126(98)00021-5)
- Kleinman, M.E., K. Yamada, A. Takeda, V. Chandrasekaran, M. Nozaki, J.Z. Baffi, R.J. Albuquerque, S. Yamasaki, M. Itaya, Y. Pan, et al. 2008. Sequence- and target-independent angiogenesis suppression by siRNA via TLR3. *Nature.* 452:591–597. <http://dx.doi.org/10.1038/nature06765>
- Lee, J., H.K. Kim, Y.M. Han, and J. Kim. 2008. Pyruvate kinase isozyme type M2 (PKM2) interacts and cooperates with Oct-4 in regulating transcription. *Int. J. Biochem. Cell Biol.* 40:1043–1054. <http://dx.doi.org/10.1016/j.biocel.2007.11.009>
- Love, K.T., K.P. Mahon, C.G. Levins, K.A. Whitehead, W. Querbes, J.R. Dorkin, J. Qin, W. Cantley, L.L. Qin, T. Racie, et al. 2010. Lipid-like materials for low-dose, in vivo gene silencing. *Proc. Natl. Acad. Sci. USA.* 107:1864–1869. <http://dx.doi.org/10.1073/pnas.0910603106>
- Mazurek, S. 2011. Pyruvate kinase type M2: A key regulator of the metabolic budget system in tumor cells. *Int. J. Biochem. Cell Biol.* 43:969–980. <http://dx.doi.org/10.1016/j.biocel.2010.02.005>
- Michelakis, E.D., G. Sutendra, P. Dromparis, L. Webster, A. Haromy, E. Niven, C. Maguire, T.L. Gammer, J.R. Mackey, D. Fulton, et al. 2010. Metabolic modulation of glioblastoma with dichloroacetate. *Sci. Transl. Med.* 2:31ra34. <http://dx.doi.org/10.1126/scitranslmed.3000677>
- Noguchi, T., H. Inoue, and T. Tanaka. 1986. The M1- and M2-type isozymes of rat pyruvate kinase are produced from the same gene by alternative RNA splicing. *J. Biol. Chem.* 261:13807–13812.
- Semenza, G.L. 2011. Regulation of Metabolism by Hypoxia-Inducible Factor 1. *Cold Spring Harb. Symp. Quant. Biol.* In press. <http://dx.doi.org/10.1101/sqb.2011.76.010678>
- Shi, H.S., D. Li, J. Zhang, Y.S. Wang, L. Yang, H.L. Zhang, X.H. Wang, B. Mu, W. Wang, Y. Ma, et al. 2010. Silencing of pkm2 increases the efficacy of docetaxel in human lung cancer xenografts in mice. *Cancer Sci.* 101:1447–1453. <http://dx.doi.org/10.1111/j.1349-7006.2010.01562.x>
- Ugurel, S., N. Bell, A. Sucker, A. Zimpfer, W. Rittgen, and D. Schadendorf. 2005. Tumor type M2 pyruvate kinase (TuM2-PK) as a novel plasma tumor marker in melanoma. *Int. J. Cancer.* 117:825–830. <http://dx.doi.org/10.1002/ijc.21073>
- Vander Heiden, M.G., L.C. Cantley, and C.B. Thompson. 2009. Understanding the Warburg effect: the metabolic requirements of cell proliferation. *Science.* 324:1029–1033. <http://dx.doi.org/10.1126/science.1160809>
- Vander Heiden, M.G., H.R. Christofk, E. Schuman, A.O. Subtelny, H. Sharfi, E.E. Harlow, J. Xian, and L.C. Cantley. 2010a. Identification of small molecule inhibitors of pyruvate kinase M2. *Biochem. Pharmacol.* 79:1118–1124. <http://dx.doi.org/10.1016/j.bcp.2009.12.003>
- Vander Heiden, M.G., J.W. Locasale, K.D. Swanson, H. Sharfi, G.J. Heffron, D. Amador-Noguez, H.R. Christofk, G. Wagner, J.D. Rabinowitz, J.M. Asara, and L.C. Cantley. 2010b. Evidence for an alternative glycolytic pathway in rapidly proliferating cells. *Science.* 329:1492–1499. <http://dx.doi.org/10.1126/science.1188015>
- Wang, E.T., R. Sandberg, S. Luo, I. Khrebtkova, L. Zhang, C. Mayr, S.F. Kingsmore, G.P. Schroth, and C.B. Burge. 2008a. Alternative isoform regulation in human tissue transcriptomes. *Nature.* 456:470–476. <http://dx.doi.org/10.1038/nature07509>
- Wang, Y., G. Sheng, S. Juraneck, T. Tuschl, and D.J. Patel. 2008b. Structure of the guide-strand-containing argonaute silencing complex. *Nature.* 456:209–213. <http://dx.doi.org/10.1038/nature07315>
- Warburg, O. 1956. On the origin of cancer cells. *Science.* 123:309–314. <http://dx.doi.org/10.1126/science.123.3191.309>